THE JOURNAL OF PHYSICAL CHEMISTRY B

Article

pubs.acs.org/JPCB

Excited-State Proton and Charge Transfer in Protonated Amino and Methylated Derivatives of 2-(2′-Hydroxyphenyl)benzimidazole

Sonia Ríos Vázquez, J. Luis Pérez Lustres, Flor Rodríguez-Prieto,* Manuel Mosquera,* and M. Carmen Ríos Rodríguez*

Departamento de Química Física and Centro Singular de Investigación en Química Biolóxica e Materiais Moleculares (CIQUS), Universidade de Santiago de Compostela, E-15782 Santiago de Compostela, Spain

ABSTRACT: We studied the excited-state behavior of a family of mono- and diprotonated derivatives of 2-phenylbenzimidazole in different solvents, using steady-state and time-resolved fluorescence spectroscopy. The species investigated were 2-(4′-amino-2′-hydroxyphenyl)benzimidazole (**1**), the diethylamino analogue 2-(4′-*N*,*N*-diethylamino-2′-hydroxyphenyl)-benzimidazole (**2**) and its *N*-methylated derivative 1-methyl-2-(4′-*N*,*N*-diethylamino-2′-hydroxyphenyl)benzimidazole (**3**). The O-methoxy derivatives of **2** and **3** (**2-OMe** and **3-OMe**), and the simpler models 2-phenylbenzimidazole (**4**) and its 4′-amino (**5**) and 4′-dimethylamino (**6**) derivatives were also studied. We found that the dications of **1**, **2**, and **3** (protonated at the benzimidazole N3 and at the amino group) were strong photoacids, which were deprotonated at the hydroxyl group upon excitation in aqueous solution (totally for **2** and **3**) to give a tautomer of the ground-state monocation. In contrast, no photodissociation was observed for the monocations of these species. Instead, some of the monocations studied behaved as molecular rotors, for which electronic excitation led to a twisted intramolecular charge transfer (TICT) state. The monocations of **2**, **3**, **2-OMe**, **3-OMe**, and **6**, protonated at the benzimidazole N3, experienced a polarity- and viscosity-dependent radiationless deactivation associated with a large-amplitude rotational motion. We propose that this process is connected to an intramolecular charge transfer from the dimethylaminophenyl or diethylaminophenyl moiety (donor) to the protonated benzimidazole group (acceptor) of the excited monocation, which yields a twisted charge-transfer species. No fluorescence from this species was detected except for **3** and **3-OMe** in low-viscosity solvents.

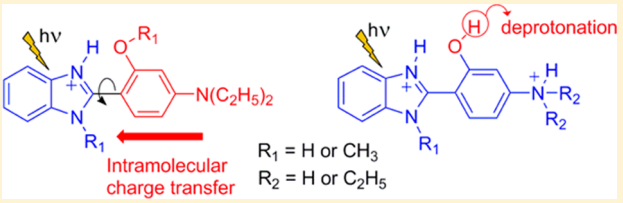

1. INTRODUCTION

Proton- and electron-transfer reactions, frequently coupled, play a crucial role in many essential processes taking place in living organisms, like DNA chemical damage and repair,[1,2] photostability of DNA base pairs and proteins,[3] photosynthesis,[4] and respiration.[5] Although these reactions have been extensively investigated, the detailed mechanisms of charge transfer and proton motion, and in particular, the coupling between them, are not completely understood.[6−11]

Photoinduced proton- and electron-transfer processes are triggered by the change of acid−base and redox properties of molecules upon electronic excitation. Molecules with both electron donor and acceptor moieties often undergo in the excited state a photoinduced intramolecular electron transfer. These systems have applications as luminescence sensors,[12] in organic solar cells,[13,14] or in light-driven molecular machines.[15]

Molecules with increased acidity in the excited state are called photoacids, as they have the tendency to be deprotonated upon excitation in solvents capable of accepting the proton or in the presence of basic species. Recent research on photoacids has greatly contributed to our understanding of the elementary steps in proton-transfer processes.[16−19] Photoacids have also found applications as polymerization initiators,[20] in molecular machines[21] and in pH-jump experiments.[22] If a molecule has an acid group and a basic site linked by a hydrogen bond in the ground state, an ultrafast excited-state intramolecular proton transfer, ESIPT, from the acid to the basic site may occur. ESIPT molecules have technological applications as UV photostabilizers[23] and are potential components for photoswitches[24] and organic LEDs.[25]

2-(2′-Hydroxyphenyl)benzimidazole (HBI),[26−40] 2-(4′-amino-2′-hydroxyphenyl)benzimidazole (**1**),[36,41,42] 2-(4′-*N*,*N*-diethylamino-2′-hydroxyphenyl)benzimidazole (**2**),[36,41] 1-methyl-2-(4′-*N*,*N*-diethylamino-2′-hydroxyphenyl)-benzimidazole (**3**),[41] and 2-(3′-hydroxy-2′-pyridyl)-benzimidazole[43,44] are examples of ESIPT molecules studied in our group (see Chart 1). A solvent-modulated ground-state rotameric and tautomeric equilibrium was observed for these benzimidazole derivatives. In apolar aprotic solvents, these compounds exist in the ground state as the planar *syn* normal form $\mathbf{N}_{syn}$ (Chart 1), with an intramolecular hydrogen bond N···H−O. This species undergoes in the first-excited singlet state an intramolecular proton transfer from the hydroxyl group to the benzimidazole N3 to yield the excited **T** tautomer (see in

Special Issue: Photoinduced Proton Transfer in Chemistry and Biology Symposium

Received: August 5, 2014
Revised: September 13, 2014

dx.doi.org/10.1021/jp507917u | *J. Phys. Chem. B* XXXX, XXX, XXX−XXX

Chart 1. Molecular Structures of the Neutral Isomers of HBI, 1, 2, and 3; Normal Forms (N_{syn}, N_{anti}, N_{np}), and the Tautomer T Obtained after ESIPT Are Shown

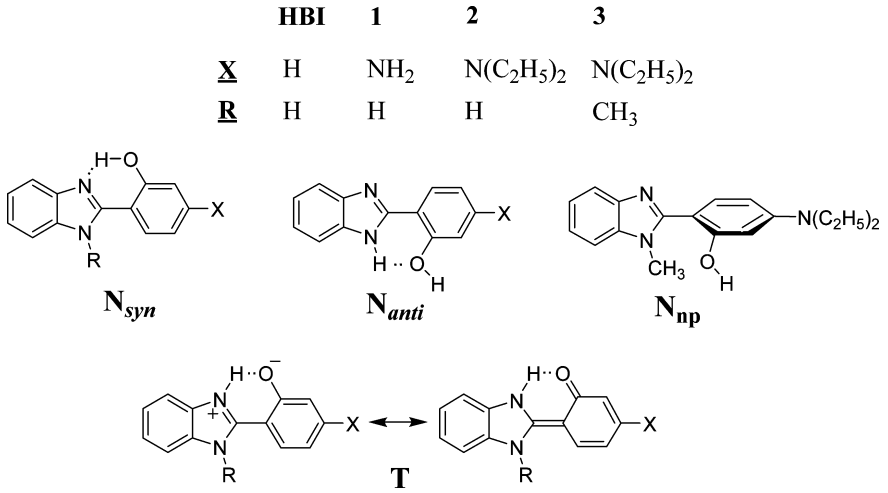

Chart 2. Molecular Structures of the Monocations (MC) Studied in this Work, Ordered as a Function of the Electron-Donor Strength of the Phenyl Moiety and the Steric Interactions of the Aromatic Rings

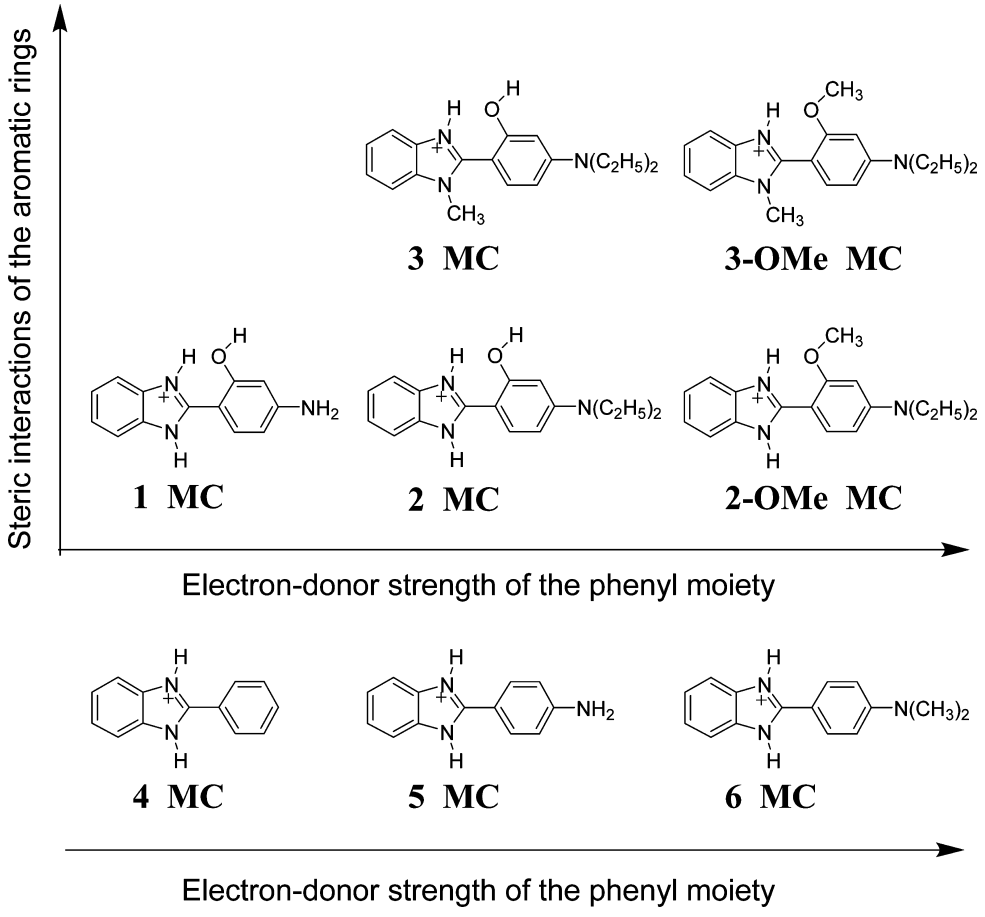

Chart 1 the limiting resonance structures of this species). In protic solvents, a ground-state rotameric equilibrium between N_{syn} and its planar *anti* rotamer N_{anti} was detected for HBI,[31,32,34] **1**, and **2**, and between N_{syn} and a nonplanar N_{np} rotamer for the sterically hindered compound **3** (Chart 1).[41] N_{anti} and N_{np}, unable to undergo ESIPT, yield normal N* emission upon excitation. Water stabilizes the ground-state **T** tautomer, which was detected by its red-shifted absorption in aqueous solutions of HBI, **1**, **2**, and **3**.[34,41]

Whereas the fluorescence quantum yield and lifetime of **T*** showed for HBI no dependence on solvent or temperature,[45] those of the tautomers of **2** and **3** revealed a temperature-, polarity-, and viscosity-dependent radiationless deactivation connected with a large-amplitude conformational motion occurring for these HBI derivatives.[41] We have shown that

dx.doi.org/10.1021/jp507917u | J. Phys. Chem. B XXXX, XXX, XXX–XXX

this conformational change is associated with a charge transfer experienced by **T*** from the deprotonated dialkylaminophenol group (donor) to the protonated benzimidazole group (acceptor), affording a nonfluorescent charge-transfer structure $\mathbf{T}^*_{ct}$.[41] This excited-state intramolecular proton-coupled charge-transfer process was reported by us for 2-(2′-hydroxyphenyl)-benzoxazole, 2-(2′-hydroxyphenyl)benzothiazole, and other hydroxyarylbenzazoles in solution, but we did not observe it for HBI.[45] We demonstrated that the efficiency of this process increased with the electron-donor strength and with the steric hindrance caused by N1-methylation, and decreased as the solvent viscosity was increased. Theoretical calculations performed later by Tsai et al.[36] on HBI, **1**, and **2** predict that two different charge-transfer states are stable in ethanol and cyclohexane for these compounds. Recently reported investigations[37] on ESIPT in crystal structures of HBI polymorphs (α and β) showed that the tautomer form of polymorph β undergoes in the excited state an intramolecular charge transfer process which does not occur for polymorph α, revealing the importance of intermolecular interactions for the relative stability of **T*** and its charge-transfer form. In a poly(methyl methacrylate) film, the polarizability of HBI tautomer was found to be smaller in S_1 than in S_0, suggesting a twisted geometry for **T** in S_1.[38] Molecules showing a viscosity-dependent fluorescence lifetime due to an intramolecular twisting occurring in the excited state are molecular rotors. These fluorescent molecular rotors can be employed as reporters of the local microviscosity, in particular in live cells, by fluorescence lifetime imaging.[46,47]

We found that the monocations of HBI,[34] 2-(3′-hydroxy-2′-pyridyl)benzimidazole,[48] and 2-(1′-hydroxy-2′-naphthyl)-benzimidazole,[19,49] protonated at the benzimidazole N3, are strong photoacids, which become completely deprotonated at the OH group in aqueous solution and to a great extent in short-chain alcohols. It is interesting to investigate the effect of the electron-donating substituents at the phenol group on the photoacid properties of this class of compounds. The amino groups of **1**, **2**, and **3** act as electron donors, but this effect disappears when they are protonated. We will study the influence of a protonated or nonprotonated amino group on the photoacid behavior for the monocations (**MC**, see Chart 2) and dications (**DC**) of **1**, **2**, and **3**.

If we compare the monocations of **1**, **2**, and **3** (Chart 2) with the structure of the neutral tautomer **T** (Chart 1), we observe that they have the same electron acceptor (protonated benzimidazole), but the monocations have a weaker electron donor (aminophenol instead of aminophenoxy group). Therefore, it is also possible that the excited monocations undergo a charge-transfer process from the aminophenol group to the protonated benzimidazole moiety. This process is also possible for the monocations of **2-OMe** and **3-OMe** (Chart 2). In contrast, the dications of **1**, **2**, **3**, **2-OMe**, and **3-OMe**, protonated both at the benzimidazole N3 and at the amino group, are not expected to undergo the photoinduced charge transfer process, as the protonated aminophenol moiety is not a good electron donor. Therefore, it is interesting to compare the behavior of monocations and dications of the mentioned species, to investigate the existence of the intramolecular charge-transfer process.

In this paper, we present a study of the ground- and excited-state behavior of the monocations and dications of **1**, **2**, and **3**, in different acidified protic and aprotic solvents. We report the room-temperature fluorescence of **1**, **2**, and **3** in acidified solvents of various viscosities and polarities and compare it with the fluorescence of the methoxy derivatives **2-OMe** and **3-OMe** (Chart 2), unable to deprotonate under excitation, but prone to undergo a charge-transfer process in the excited state. Moreover, we investigated the fluorescence of the monocations of simple models phenylbenzimidazole (**4**, Chart 2), *p*-aminophenylbenzimidazole (**5**), and *p*-dimethylaminophenyl-benzimidazole (**6**), sharing the same electron acceptor, but with different electron donors.

The aims of the present study were (1) to find out if the monocations and dications of **1**, **2**, and **3** deprotonate in the excited state in protic solvents and (2) to examine if these compounds and the related species shown in Chart 2 undergo in the excited state a large-amplitude conformational motion connected to an intramolecular charge migration analogous to that observed for the neutral tautomer **T***.

2. EXPERIMENTAL SECTION

2.1. Materials. HBI[34] and **1**, **2**, **3**, **2-OMe**, and **3-OMe**[41] were synthesized as described elsewhere. Compound **4** was provided by Aldrich.

Compound **5** was prepared by condensation of 20 mmol of 1,2-benzenediamine (Aldrich) with 20 mmol of 4-amino-benzoic acid (Aldrich) at ∼100 °C for 24 h. The solid obtained was dissolved in acetone and the product precipitated by adding water. ^{1}H NMR (300 MHz, DMSO), δ (ppm): 5.58 (s, 2H), 6.65 (d, 2H, J = 8.8 Hz), 7.10 (dd, 2H, J = 6.1 Hz, J = 3.4 Hz), 7.46 (m, 2H), 7.83 (d, 2H, J = 8.8 Hz), 12.40 (s, 1H). MS, m/z (rel. intensity): 209 (100.0, M), 118 (7.6, M − 91).

To obtain **6**, 15 mmol of 1,2-benzenediamine (Aldrich) were added to a stirred solution of 15 mmol of 4-dimethylamino-benzoic acid (Aldrich) in 25 mL of toluene at 90 °C. A total of 18 mmol of PCl_3 were then added dropwise, and the mixture was kept refluxing for 12 h. The solid obtained was repeatedly washed with toluene and the product recrystallized from ethanol. ^{1}H NMR (300 MHz, DMSO), δ (ppm): 3.05 (s, 6H), 6.90 (d, 2H, J = 8.7 Hz), 7.35 (dd, 2H, J = 3.1 Hz, J = 5.9 Hz), 7.64 (dd, 2H, J = 3.1 Hz, J = 5.9 Hz), 8.06 (d, 2H, J = 8.7 Hz). MS, m/z (rel. intensity): 237 (100.0, M), 222 (9.2, M − 15), 194 (9.2, M − 43), 119 (11.3, M − 118).

2.2. Methods. Solutions were made up in double-distilled water and spectroscopy-grade solvents, and were not degassed. Acidity was varied with $HClO_4$ in nonaqueous solutions, and with $HClO_4$, NaOH or NaH_2PO_4/Na_2HPO_4 buffer (all Merck p.a. products) in aqueous solutions. Nonaqueous solutions were either slightly acidified or strongly acidified to have the compounds in the ground state as the monocations or the dications, respectively, as confirmed by UV−vis absorption spectroscopy and comparison with the well-known spectra of the cations in aqueous solutions. Sample concentrations of $\sim 10^{-5}$ mol dm^{-3} for absorption and $\sim 10^{-6}$ mol dm^{-3} for fluorescence were employed. All experiments were carried out at 25 °C.

pH was measured with a Radiometer PHM 82 pH meter equipped with a Radiometer Type B combined electrode. Reported pK_a are practical values obtained from pH measurements and concentrations of acid and base, measured from the absorption spectra. They are not corrected to obtain the true thermodynamic values.

UV−vis absorption spectra were recorded in a Varian Cary 3E spectrophotometer. Fluorescence excitation and emission spectra were recorded in a Spex Fluorolog-2 FL340 E1 T1 spectrofluorometer, with correction for instrumental factors by

dx.doi.org/10.1021/jp507917u | J. Phys. Chem. B XXXX, XXX, XXX−XXX

means of a Rhodamine B quantum counter and correction files supplied by the manufacturer. Fluorescence quantum yields were measured using quinine sulfate ($<3 \times 10^{-5}$ mol dm^{-3}) in aqueous H_2SO_4 (0.5 mol dm^{-3}) as standard (ϕ = 0.546).[50,51] The estimated standard uncertainty of the fluorescence quantum yields measurements was 5%. Fluorescence lifetimes were determined by single-photon timing in an Edinburgh Instruments FL-900 spectrometer equipped with a hydrogen-filled nanosecond flashlamp and the reconvolution analysis software supplied by the manufacturer.

Model equations were fitted to the experimental data by means of a nonlinear weighted least-squares routine based on the Marquardt algorithm. The reported uncertainties represent the statistical standard deviations obtained in the fits.

3. RESULTS

3.1. Absorption Spectra of 1, 2, 3, 2-OMe, and 3-OMe in Aqueous Solutions. The absorption spectra of **1** in aqueous solutions under neutral and acidic conditions are shown in Figure 1a. The absorption spectrum of **1** in neutral medium showed an intense band at 31000 cm^{-1} and a weaker band at ~27000 cm^{-1}. On decreasing the pH from neutral solution, the absorption spectrum shifted to the red and its molar absorption coefficient increased with respect to that observed under neutral conditions. A new spectrum, peaking at 29320 cm^{-1}, was observed at pH 3.02. A further decrease of pH strongly shifted the absorption spectrum to the blue, the molar absorption coefficient decreasing to less than half its value at pH ~ 3. The absorbance−pH data of **1** at 35710 cm^{-1} and at 27780 cm^{-1} are given in the inset of Figure 1a.

The absorption spectra obtained for **2** and the methoxy derivative **2-OMe** in aqueous solutions at different acidities (Figure 1b,c) showed the same general features as those of **1**. The absorption spectrum recorded for **2-OMe** at pH ~ 10 showed, however, only one band similar in shape and position to the intense absorption band obtained for **1** and **2** under neutral conditions. The absorbance−pH curves were similar for **1**, **2**, and **2-OMe** (insets of Figure 1).

The absorption spectra of **3** and the methoxy derivative **3-OMe** in aqueous solutions at different acidities are shown in Figure 2. The absorption spectrum of **3** under neutral conditions, peaking at 30500 cm^{-1}, was very broad (Figure 2a). Upon acidifying the solution (pH ~ 5), the spectrum shifted to the red (maximum at 28740 cm^{-1}) and the molar absorption coefficient significantly increased. A further increase of acidity strongly shifted the spectrum to the blue, and a new band, peaking at 35460 cm^{-1}, was obtained at [$HClO_4$] ~ 0.7 mol dm^{-3}, its maximum molar absorption coefficient decreasing to about half the value obtained for the absorption spectrum recorded at pH ~ 5. Furthermore, increasing the pH from neutral conditions caused a blue shift of the spectrum, a new band being obtained at pH > 10 (results not shown). On the other hand, the absorption spectrum recorded for **3-OMe** in aqueous solutions under strongly ([$HClO_4$] = 0.1 mol dm^{-3}) and mildly (pH ~5) acidic conditions were very similar to those obtained for **3**. Upon increasing the pH from pH 5, the absorption spectrum of **3-OMe** strongly shifted to the blue, and a new band (peaking at 32150 cm^{-1}) was obtained at pH > 8, this absorption spectrum being ~1600 cm^{-1} blue-shifted with respect to that measured for **3** at pH ~ 8. The insets of Figure 2a,b show the absorbance−pH data for compounds **3** and **3-OMe**.

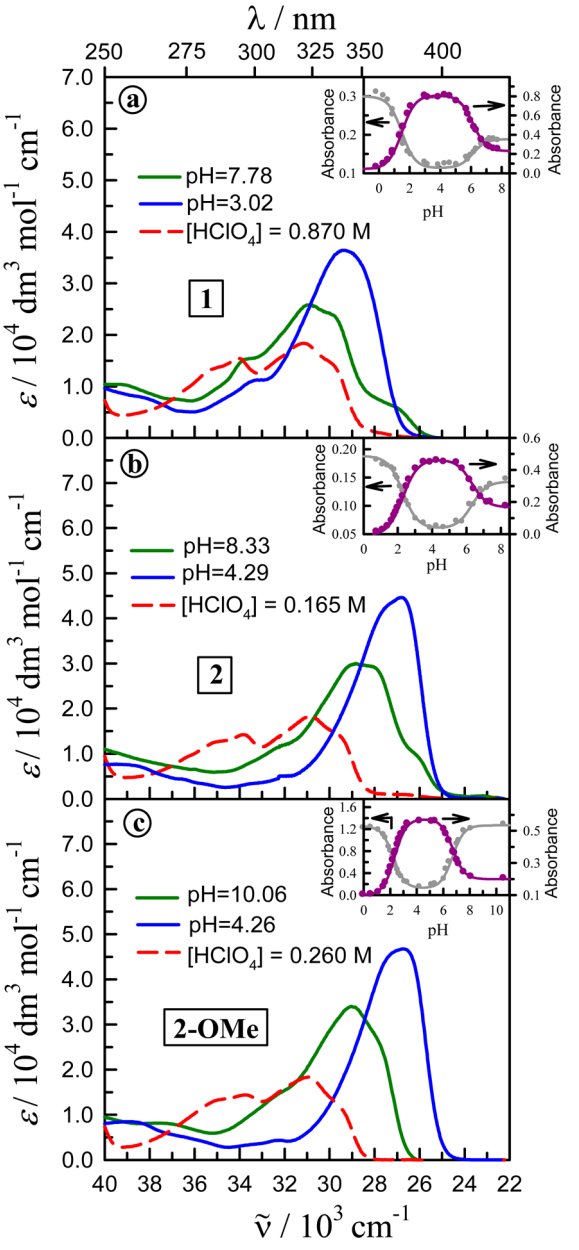

Figure 1. Absorption spectra of (a) **1**, (b) **2**, and (c) **2-OMe** in neutral, mildly acidic, and strongly acidic aqueous solution. The insets show the pH dependence of the absorbance in aqueous solution (a) for **1** at 27780 cm^{-1} (purple circle) and at 35710 cm^{-1} (gray circle); (b) for **2** at 27030 cm^{-1} (purple circle) and at 31250 cm^{-1} (gray circle); and (c) for **2-OMe** at 27030 cm^{-1} (purple circle) and at 31250 cm^{-1} (gray circle).

3.2. Fluorescence Spectra, Quantum Yields, and Lifetimes of 1, 2, 3, 2-OMe, 3-OMe, 5, and 6 in Various Solvents under Strongly Acidic Conditions (Ground-State Diprotonated Species). The fluorescence spectra of **1**, **2**, **2-OMe**, **3**, and **3-OMe** in strongly acidified aqueous solution and acetonitrile (where the ground-state species are the dications **DC**, see later) are shown in Figure 3. The fluorescence spectra of **1**, **2**, and **3** exhibited the same general features, and the excitation spectra matched the first absorption band measured under the same conditions. The emission spectra of **2** and **3** in water showed only one band (at about 23000 cm^{-1} and 22000 cm^{-1}, respectively) strongly red-shifted

dx.doi.org/10.1021/jp507917u | J. Phys. Chem. B XXXX, XXX, XXX−XXX

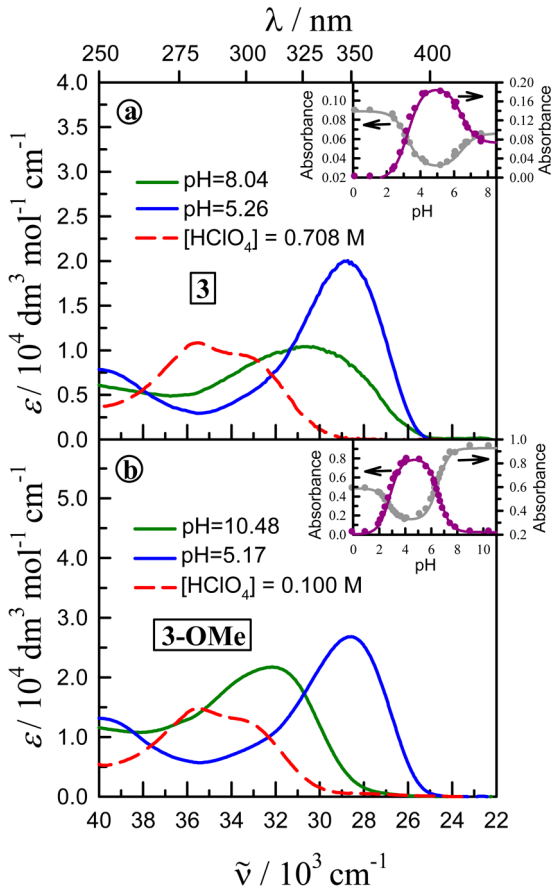

Figure 2. Absorption spectra of (a) **3** and (b) **3-OMe** in neutral, mildly acidic, and strongly acidic aqueous solution. The insets show the pH dependence of the absorbance (a) for **3** at 28570 cm^{-1} (purple circle) and at 34480 cm^{-1} (gray circle), and (b) for **3-OMe** at 27030 cm^{-1} (purple circle) and at 33330 cm^{-1} (gray circle).

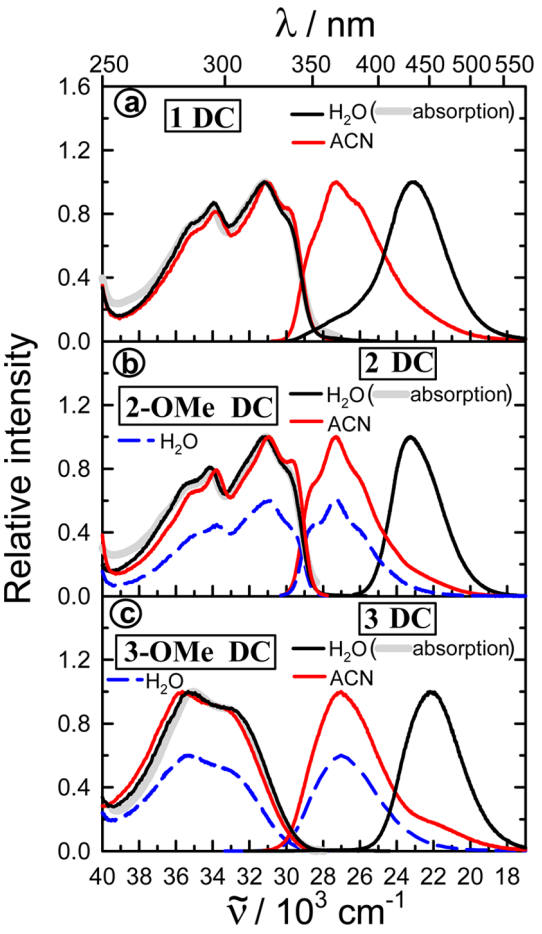

Figure 3. Normalized fluorescence excitation and emission spectra in strongly acidified solutions of (a) **1** in acetonitrile ($\tilde{\nu}_{exc}$ = 31060 cm^{-1}, $\tilde{\nu}_{em}$ = 27250 cm^{-1}) and water ($\tilde{\nu}_{exc}$ = 31150 cm^{-1}, $\tilde{\nu}_{em}$ = 22990 cm^{-1}), (b) **2** in acetonitrile ($\tilde{\nu}_{exc}$ = 30770 cm^{-1}, $\tilde{\nu}_{em}$ = 27400 cm^{-1}) and water ($\tilde{\nu}_{exc}$ = 30770 cm^{-1}, $\tilde{\nu}_{em}$ = 23260 cm^{-1}), and **2-OMe** in water ($\tilde{\nu}_{exc}$ = 30860 cm^{-1}, $\tilde{\nu}_{em}$ = 27170 cm^{-1}), and (c) **3** in acetonitrile ($\tilde{\nu}_{exc}$ = 35650 cm^{-1}, $\tilde{\nu}_{em}$ = 27030 cm^{-1}) and water ($\tilde{\nu}_{exc}$ = 35340 cm^{-1}, $\tilde{\nu}_{em}$ = 22200 cm^{-1}), and **3-OMe** in water ($\tilde{\nu}_{exc}$ = 35460 cm^{-1}, $\tilde{\nu}_{em}$ = 27030 cm^{-1}). The absorption spectra of **1**, **2**, and **3** in aqueous solution of the same pH as that of the fluorescence spectra are also shown (gray band).

with respect to its excitation spectrum. However, for **1** the main emission band (at 23000 cm^{-1}) was accompanied by a shoulder at about 27000 cm^{-1}, which overlapped its excitation spectrum. In acidified acetonitrile, the emission spectra of **1**, **2**, and **3**, located at about 27000 cm^{-1}, were very similar to those recorded for **2-OMe** and **3-OMe** in acidified aqueous solution, except for a weak emission observed at ~22000 cm^{-1}, not detected for the methoxy derivatives. The fluorescence quantum yields Φ_{DC} of the species studied in this work in different strongly acidified solvents are given in Table 1.

The fluorescence of **2-OMe** exhibited monoexponential decays both in aqueous solution and acetonitrile, with the same lifetime (1.7 ns, Table 2). A monoexponential decay was also observed for **2** in aqueous solution at 23260 cm^{-1}, with a lifetime of 3.8 ns. In acetonitrile, the fluorescence decay was monoexponential at the main emission band (in the range 24390 cm^{-1} to 28570 cm^{-1}) with a lifetime of 1.5 ns and became biexponential at lower wavenumbers with lifetimes of 1.5 and 4.0 ns (at 23260 cm^{-1}, see Table 2).

3.3. Fluorescence Spectra, Quantum Yields, and Lifetimes of 1, 2, 3, 2-OMe, 3-OMe, 4, 5, and 6 in Various Solvents under Mildly Acidic Conditions (Ground-State Monoprotonated Species). The fluorescence spectra of **1** in mildly acidified aqueous solution and acetonitrile (where the ground-state species exist as monocations, see later) are shown in Figure 4a. The excitation and emission spectra of **1** were independent of the monitoring wavenumbers both in acidified aqueous solution and acetonitrile. The emission spectrum in aqueous solution of pH 3.71 showed only one band, located at 25220 cm^{-1}, which overlapped its excitation spectrum. This spectrum, peaking at 28450 cm^{-1}, coincided with the absorption spectrum of **1** measured under the same acidity conditions. The fluorescence excitation spectrum of **1** measured in slightly acidified acetonitrile overlapped its emission band and the emission spectrum almost matched that observed in acidic aqueous solution.

The fluorescence behavior observed for **2** (Figure 4b) was very similar to that of **1** (Figure 4a). The excitation and emission spectra of **2-OMe** in acidified water were also independent of the monitoring wavenumbers, and, except for a small red shift, showed the same features as the excitation and emission bands recorded for **2** in the same solvent (Figure 4b).

The fluorescence spectra of **3** and **3-OMe** in slightly acidified acetonitrile are shown in Figure 4c. For both compounds, the excitation spectrum virtually matched the absorption spectrum measured under the same acidity conditions, and the emission

dx.doi.org/10.1021/jp507917u | J. Phys. Chem. B XXXX, XXX, XXX–XXX

Table 1. Fluorescence Quantum Yields Φ_{DC} of the Dications of the Species Studied in this Work at 298 K in Various Strongly Acidified Solvents, for Which the Viscosity and the Relative Dielectric Permittivity Are Shown

			Φ_{DC}						
solvent	ε_r[a]	η[b] /cP	5	6	1	2	2-OMe	3	3-OMe
dioxane	2.21	1.44					0.42	0.38	
diethyl ether	4.20	0.24		0.42					
ethyl acetate	6.02	0.45		0.27		0.37	0.55		
tetrahydrofuran	7.58	0.55		0.13			0.38		0.26
acetonitrile	35.94	0.36	0.54	0.42	0.23		0.50	0.60	0.14
1-octanol	10.30	10.64		0.25			0.43		0.24
2-butanol	16.56	4.21		0.23			0.43		
ethanol	24.55	1.20		0.28			0.46		0.26
methanol	32.66	0.55		0.18			0.46		
water	78.30	1.00	0.32	0.39			0.41		
ethylene glycol	37.70	19.90		0.21			0.40		
glycerol	42.50	1412		0.19					

[a]Values at 298.15 K from ref 75. [b]Values at 298.15 K from ref 76.

Table 2. Fluorescence Lifetimes τ_1 and τ_2 and Associated Fractional Intensities (in Square Brackets) of 2 and 2-OMe in Acetonitrile and Water under Excitation of Dication DC in Strongly Acidic Conditions at 298 K; The Species to Which Each Lifetime Was Assigned Are Also Shown

compound	$\tilde{\nu}_{exc}$ /cm^{-1}	$\tilde{\nu}_{em}$ /cm^{-1}	τ_1 /ns	τ_2 /ns	χ^2
			Strongly Acidified Acetonitrile		
2 DC	30770	28570	1.522 ± 0.005 (**DC***)		1.038
	30770	24390	1.587 ± 0.005 (**DC***)		1.153
	30770	23260	1.5[a] [52%] (**DC***)	4.05 ± 0.04 [48%] (**TC***)	1.092
2-OMe DC	31250	27030	1.744 ± 0.003 (**DC***)		1.018
	31250	23810	1.755 ± 0.003 (**DC***)		1.124
			Strongly Acidified Aqueous Solution		
2 DC	30770	23260	3.812 ± 0.002 (**TC***)		1.072
2-OMe DC	33330	25974	1.679 ± 0.004 (**DC***)		1.022
	33330	24390	1.714 ± 0.004 (**DC***)		1.092

[a]Fixed value, obtained at emission wavenumbers where the decay is monoexponential. Fixing this value, a more precise value of τ_2 is obtained at this wavenumber.

spectrum overlapped its excitation spectrum. The fluorescence emission bands of **3** and **3-OMe** were much broader than the emission bands recorded for **1**, **2**, and **2-OMe** in the same solvent. The emission spectrum of **3-OMe** in acidified glycerol was however narrower than those recorded for **3** and **3-OMe** in acetonitrile (Figure 4c).

The absorption and fluorescence spectra of the model compounds **4**, **5**, and **6** in slightly acidified acetonitrile (so as to have all these compounds as the monocations) are shown in Figure 4d. For all compounds, the excitation spectrum matches the first absorption band and the emission spectrum overlaps its excitation spectrum. Also, a red shift of both the excitation and emission spectra is observed on going from **4** to **5** and from **5** to **6**.

The fluorescence quantum yields Φ_{MC} of the monocationic species studied in this work, obtained in different mildly acidified solvents, are compiled in Table 3. It is observed that the quantum yields of **1** were similar to those of the model compound HBI, without the amino group. However, the values measured for **2** were in some cases lower than those found for **1** and HBI, and the effect was clearly stronger for **2-OMe**. Furthermore, the quantum yields of **2** and **2-OMe** markedly increased with the solvent viscosity (especially for **2-OMe**) and decreased as the dielectric permittivity of the solvent increased. The fluorescence quantum yields of **3** and **3-OMe** were generally lower than those measured for **2** and **2-OMe**. The fluorescence quantum yields of the monocations of model compounds **4**, **5**, and **6**, with no hydroxyl or methoxy groups, decreased in the series **4** $\geq$ **5** $\gg$ **6**, the values decreasing up to 58 times (in acetonitrile) on going from **5** to **6**.

Table 4 shows the fluorescence decays of **1**, **2**, **2-OMe**, and **3-OMe**, and the model compounds **5** and **6**, recorded in slightly acidified acetonitrile and 1-octanol. In acetonitrile, the decay was monoexponential for **1** and **5** (lifetimes around 1.3 ns), but it became biexponential for the other derivatives (lifetimes around 1 and 0.1 ns). The intensity fraction corresponding to the short lifetime increased as the emission wavenumber decreased. For **3-OMe**, the biexponential decay obtained at 23530 cm^{-1} with lifetimes of 1.9 (5%) and 0.216 ns (95%) became monoexponential at 21740 cm^{-1} with a lifetime of 0.164 ns. In slightly acidified 1-octanol, the fluorescence decay of **2** became monoexponential (lifetime 1.28 ns), whereas **2-OMe**, **3-OMe**, and **6** exhibited biexponential decays (Table 4), with a long lifetime around 1 ns and a shorter one in the range 0.3 to 0.6 ns.

4. DISCUSSION

4.1. Ground-State Acid–Base Equilibria of 1, 2, 3, 2-OMe, and 3-OMe in Aqueous Solution: First Protonation Occurs at the Benzimidazole Nitrogen. In a previous paper, we showed that **1**, **2**, and **3** in neutral aqueous solution exhibit tautomeric equilibria between the normal form **N** and

dx.doi.org/10.1021/jp507917u | J. Phys. Chem. B XXXX, XXX, XXX–XXX

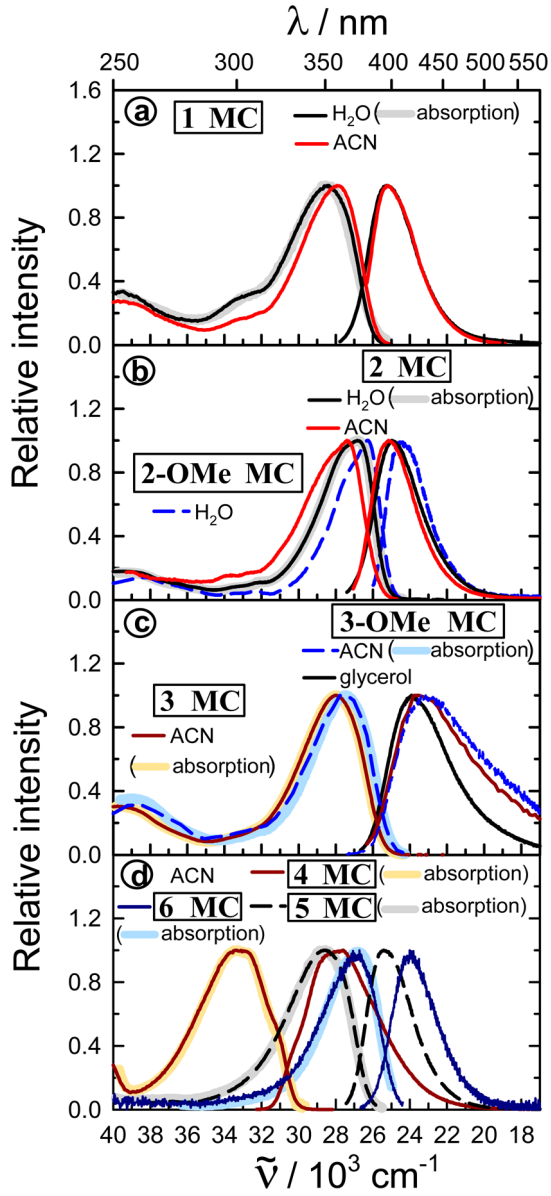

Figure 4. Absorption spectra and normalized fluorescence excitation and emission spectra of the monoprotonated forms of the indicated species in mildly acidic solutions. (a) **1** in acetonitrile ($\tilde{\nu}_{exc}$ = 27930 cm^{-1}, $\tilde{\nu}_{em}$ = 25190 cm^{-1}) and water at pH 3.71 ($\tilde{\nu}_{exc}$ = 28410 cm^{-1}, $\tilde{\nu}_{em}$ = 25190 cm^{-1}), (b) **2** in acetonitrile ($\tilde{\nu}_{exc}$ = 27400 cm^{-1}, $\tilde{\nu}_{em}$ = 25160 cm^{-1}) and water at pH 4.71 ($\tilde{\nu}_{exc}$ = 26820 cm^{-1}, $\tilde{\nu}_{em}$ = 24970 cm^{-1}) and **2-OMe** in acetonitrile ($\tilde{\nu}_{exc}$ = 26320 cm^{-1}, $\tilde{\nu}_{em}$ = 24440 cm^{-1}), (c) **3** in acetonitrile ($\tilde{\nu}_{exc}$ = 28010 cm^{-1}, $\tilde{\nu}_{em}$ = 23530 cm^{-1}) and **3-OMe** in acetonitrile ($\tilde{\nu}_{exc}$ = 28010 cm^{-1}, $\tilde{\nu}_{em}$ = 23150 cm^{-1}) and glycerol ($\tilde{\nu}_{exc}$ = 23920 cm^{-1}), and (d) **4** ($\tilde{\nu}_{exc}$ = 33330 cm^{-1}, $\tilde{\nu}_{em}$ = 27620 cm^{-1}), **5** ($\tilde{\nu}_{exc}$ = 28570 cm^{-1}, $\tilde{\nu}_{em}$ = 25380 cm^{-1}), and **6** ($\tilde{\nu}_{exc}$ = 26740 cm^{-1}, $\tilde{\nu}_{em}$ = 24040 cm^{-1}) in acetonitrile.

the tautomer **T** (see Chart 1), the last species being responsible for the red-shifted absorption band appearing at ~27000 cm^{-1}.[41] This equilibrium is impossible for **2-OMe** and **3-OMe**, which exist only as normal form **N** and lack this absorption band.

The absorption spectra of **1**, **2**, and **2-OMe** (Figure 1), as well as those of **3** and **3-OMe** (Figure 2) in aqueous solutions at different acidities indicate the existence of two acid–base equilibria for all these compounds in the pH ranges studied. A global analysis of the absorbance–pH data at different fixed wavenumbers was performed for each of the compounds investigated (insets of Figures 1 and 2), yielding the pK_a values listed in Table 5. We include also in this Table the pK_a values obtained by the same method for **4**, **5**, and **6**, some of which were already measured by other authors.[52,53] Our results indicate that the species involved in the ground-state acid–base equilibria for all compounds with an amino group in neutral-to-acid media are the neutral form, the monocation **MC**, and the dication **DC** (see Scheme 1, where for **1**, **2**, and **3**, species **T** in equilibrium with **N** has been omitted for clarity). Protonation of the neutral form to give the monocation can take place at the benzimidazole **N3** or at the amino **N**. In agreement with previous studies on **6**,[52] we propose that the first protonation occurs for all the species at the benzimidazole N3, based on the following facts:

(1) The absorption spectra of the neutral form and the monocation of **1** and **2** were red-shifted (stronger for **2** than for **1**) with respect to those of HBI (Figure 5a,b) and showed a higher molar absorption coefficient (Figure 1) than the neutral form and the monocation of HBI.[34] This reveals a more extended π-electron conjugation for the neutral and monoprotonated forms of **1** and **2** than for those of HBI, which must be due to the involvement of the nitrogen lone pair at the $-NH_2$ or $-NEt_2$ group in the resonance system. The stronger electron-donating ability of diethylaniline (E_{ox} = 0.34 V)[54] compared to that of aniline (E_{ox} = 0.54 V)[54] causes a more extended π-conjugation in **2** than in **1**. As the absorption spectra of the monocations of **2-OMe**, **3**, and **3-OMe** were very similar to those of **1** and **2** (Figures 1 and 2), we propose that the neutral form of all these species protonates also at the benzimidazole N3.

(2) The absorption spectra of the dications of **1** and **2**, for which the amino group is protonated (and therefore unable to act as an electron donor), coincided in shape and position with the absorption spectrum of the monocation of HBI (Figure 5c), suggesting a similar structure for the species involved.

(3) For both **1** and **2**, the molar absorption coefficients of the monocations were about 1.5 times higher than those of the neutral forms. In contrast, no difference was observed for HBI.[34] This must be due to the presence in the monocations of **1** and **2** of a positively charged benzimidazolium ring (better electron acceptor than the benzimidazole moiety of the neutral form), its charge withdrawing ability increasing the electron conjugation with the aminophenyl group.

The involvement of the amino nitrogen lone pair in the π system is also responsible for the differences between the pK_a values of HBI and those of its amino derivatives. It is observed in Table 5 that the pK_{a2} value increased in the order HBI < **1** < **2**. This is explained by the fact that the amino group at C4′ causes an increase of the electron density (and therefore the basicity) at the benzimidazole N3, stronger for $-NEt_2$ than for $-NH_2$. The same effect explains the pK_a increase for monocation deprotonation in the series **4** < **5** < **6** (Table 5). Besides, it is also observed that the pK_a value corresponding to protonation of the amino group was more than 2 units lower for **1** and **2** (pK_{a1}) than for aniline (pK_{a2} in Table 5). This must be due to the fact that the electron density at the amino N is much higher for aniline than for protonated **1** and **2**, as the

dx.doi.org/10.1021/jp507917u | J. Phys. Chem. B XXXX, XXX, XXX–XXX

Table 3. Fluorescence Quantum Yields Φ_{MC} of the Monocations of the Species Studied in this Work at 298 K in Various Mildly Acidified Solvents, for Which the Viscosity and the Relative Dielectric Permittivity Are Shown

			Φ_{MC}								
solvent	ε_r[a]	η[b] /cP	4	5	6	HBI	1	2	2-OMe	3	3-OMe
dioxane	2.21	1.44	0.35	0.28	0.10			0.19	0.14		
diethyl ether	4.20	0.24		0.30	0.27						
ethyl acetate	6.02	0.45			0.09	0.36		0.21	0.14		
tetrahydrofuran	7.58	0.55		0.48	0.09	0.26	0.24	0.27	0.09		0.07
acetonitrile	35.94	0.36	0.47	0.41	0.007	0.32	0.24	0.07	0.01	0.01	0.01
N,*N*-dimethylformamide	36.71	0.92		0.42	0.01						
dimethyl sulfoxide	46.45	1.99		0.47	0.015		0.24	0.12	0.02		0.01
1-octanol	10.30	10.64			0.21		0.27	0.37	0.27		0.16
2-butanol	16.56	4.21			0.12		0.33	0.49	0.21		
ethanol	24.55	1.20	0.47	0.52	0.03		0.25	0.26	0.06	0.02	0.03
methanol	32.66	0.55			0.01		0.29	0.14	0.03		
water	78.30	1.00	0.42	0.11	0.005		0.10	0.02	0.008		
ethylene glycol	37.70	19.90			0.06			0.15	0.07		
glycerol	42.50	1412			0.15			0.32	0.26		0.14

[a]Values at 298.15 K from ref 75. [b]Values at 298.15 K from ref 76.

Table 4. Fluorescence Lifetimes τ_1 and τ_2 and Associated Fractional Intensities (in Parentheses) of the Indicated Species in Slightly Acidified Acetonitrile and 1-Octanol under Excitation of Monocation MC at 298 K

compound	$\tilde{\nu}_{exc}$ /cm^{-1}	$\tilde{\nu}_{em}$ /cm^{-1}	τ_1 /ns	τ_2 /ns	χ^2
			Slightly Acidified Acetonitrile		
1 MC	27030	24390	1.340 ± 0.007		1.088
2 MC	26320	25000	1.125 ± 0.008 (74%)	0.22 ± 0.02 (26%)	1.052
	26320	24390	1.112 ± 0.007 (72%)	0.15 ± 0.02 (28%)	1.055
	26320	23260	1.148 ± 0.008 (66%)	0.17 ± 0.01 (34%)	1.084
2-OMe MC	26320	25320	1.16 ± 0.04 (10%)	0.124 ± 0.006 (90%)	1.003
	26320	24690	1.18 ± 0.04 (6%)	0.121 ± 0.005 (94%)	1.019
	26320	23810	1.13 ± 0.04 (5%)	0.092 ± 0.004 (95%)	1.128
3-OMe MC	28170	23530	1.9 ± 0.1 (5%)	0.216 ± 0.008 (95%)	1.018
	28170	21740		0.164 ± 0.007	1.009
5 MC	27030	25000	1.264 ± 0.002		1.009
6 MC	26320	25000	0.9 ± 0.1[a] (29%)	0.08 ± 0.01[a] (71%)	1.041
	26320	23810	0.9 ± 0.1[a] (13%)	0.08 ± 0.01[a] (87%)	1.072
			Slightly Acidified 1-Octanol		
2 MC	25970	24390	1.275 ± 0.003		1.024
	25970	22220	1.294 ± 0.003		1.123
2-OMe MC	25640	24100	1.078 ± 0.006 (86%)	0.31 ± 0.03 (14%)	1.001
	25640	22730	1.098 ± 0.008 (83%)	0.37 ± 0.04 (17%)	1.084
3-OMe MC	27780	25320	1.20 ± 0.01 (55%)	0.47 ± 0.02 (45%)	1.040
	27780	22220	1.22 ± 0.01 (78%)	0.54 ± 0.05 (22%)	1.186
6 MC	26320	25000	1.1 ± 0.1[a] (51%)	0.6 ± 0.1[a] (49%)	1.185
	26320	23810	1.1 ± 0.1[a] (44%)	0.6 ± 0.1[a] (56%)	1.022
	26320	22470	1.1 ± 0.1[a] (45%)	0.6 ± 0.1[a] (55%)	1.039

[a]Global fit.

electron density is displaced toward the protonated benzimidazole ring.

The basicity at benzimidazole N3 increases with OH substitution at C2′, as shows the pK_a increase on going from **4** to HBI and from **5** to **1** (pK_{a2} in Table 5). This effect is stronger for the methoxy group, as evidenced by the higher pK_{a2} values for the methoxy derivatives **2-OMe** and **3-OMe** than for the hydroxy compounds **2** and **3** (Table 5). These results indicate that the OH and OMe groups at the ortho position of the phenyl ring increase the electron density at the benzimidazole **N**, this effect being stronger for OMe than for OH.

The experimental pK_a values allow us to arrange the substituent groups of the phenyl moiety according to their electron-donor capacity to the benzimidazole unit. This is depicted in Chart 2, together with the relative steric interactions of the aromatic rings.

4.2. Excited-State Behavior of 1, 2, 3, 2-OMe, and 3-OMe in Strongly Acidic Solutions: Photodissociation of the Dication DC* at the Hydroxyl Group. The fluorescence excitation spectrum of **1**, **2**, and **3** in strongly acidic aqueous solution and acetonitrile (Figure 3) can be attributed to the dication **DC**, as it matched for each compound the absorption spectrum of **DC** recorded in the same acidity conditions. Likewise, the fluorescence excitation spectrum of **2-OMe** and

dx.doi.org/10.1021/jp507917u | J. Phys. Chem. B XXXX, XXX, XXX−XXX

Table 5. Acidity Constants Obtained for the Compounds Studied in this Work and Some Simple Model Compounds in Aqueous Solution at 298 K

compound	pK_{a1} **DC** ⇌ **MC**	pK_{a2} **MC** ⇌ **N**
1	1.50 ± 0.01	6.11 ± 0.02
2	2.29 ± 0.01	6.31 ± 0.02
2-OMe	2.34 ± 0.02	6.74 ± 0.02
3	3.25 ± 0.01	6.44 ± 0.03
3-OMe	2.85 ± 0.06	6.60 ± 0.01
HBI		5.48 ± 0.09[a]
4		4.95 ± 0.05
5	1.48 ± 0.01	5.95 ± 0.02
6	1.50 ± 0.01	6.11 ± 0.02
benzimidazole		5.53[b]
aniline		4.63[c]
N,*N*-diethylaniline		5.15[c]

[a]Value from ref 34. [b]Value from ref 77. [c]Values from ref 76.

3-OMe in strongly acidic aqueous solution (Figure 3b,c) is attributed to the dication, as it is very similar to the absorption band of **DC** in the same solvent (Figures 1c and 2b). The absorption and fluorescence excitation spectra shown in Figure 3 reveal a great similarity of the spectra for **1**, **2**, and **2-OMe**, and a blue shift of the spectra for **3** and **3-OMe** with respect to those of the other compounds. This behavior can be explained by assuming that the methyl group at benzimidazole N1 in **3** and **3-OMe** greatly enhances the steric hindrance between adjacent ring systems, causing the dications of **3** and **3-OMe** to be nonplanar, $\mathbf{DC}_{np}$. The loss of conjugation in $\mathbf{DC}_{np}$ would result in a blue shift of its absorption and excitation spectrum with respect to the planar form **DC** of **1**, **2**, and **2-OMe**, and a change in the shape of the spectrum. Similar results were obtained for other methylated benzimidazole derivatives.[55,56]

The fluorescence spectra in strongly acidified solutions shown in Figure 3 reveal a similar behavior for **1**, **2**, and **3** in acetonitrile, and for **2-OMe** and **3-OMe** in water, only a greater Stokes shift being detected for **3** and **3-OMe**. A completely different emission spectrum is nevertheless observed for **1**, **2**, and **3** in water, which will be discussed later.

Under excitation of **DC** in acetonitrile for **1** and **2**, and in water for **2-OMe**, a single emission band overlapping its excitation spectrum was observed (Figure 3), which we assign to **DC***. For the dications of **3** in acetonitrile and **3-OMe** in water, the emission spectrum was located in the same position as that detected for the dications of **1**, **2**, and **2-OMe**, showing only some loss of structure. This result contrasts with the absorption and excitation spectra, which were clearly blue-shifted for **3** and **3-OMe**, as discussed above. This causes that for **3** and **3-OMe** the emission spectrum of the dication hardly overlaps its excitation band, and the Stokes shift is very large.

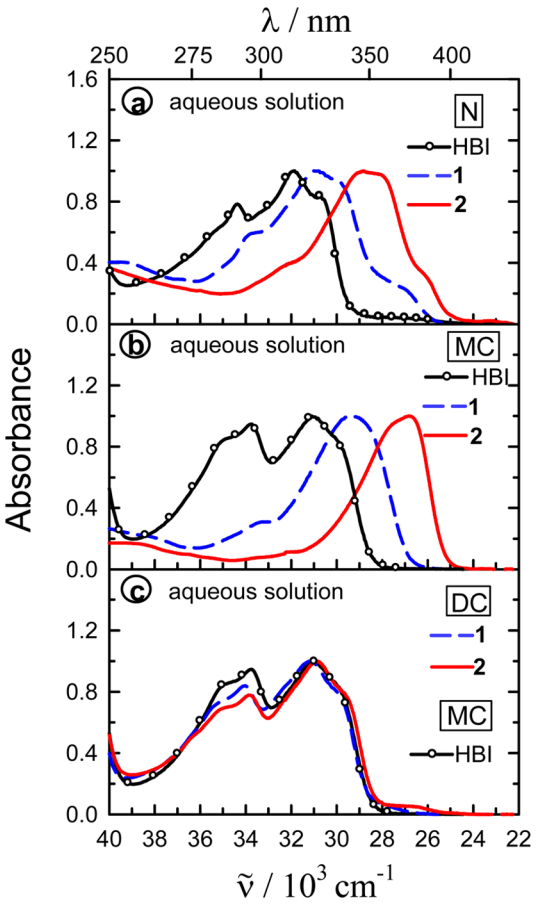

Figure 5. Normalized absorption spectra in aqueous solution of (a) the neutral forms, (b) the monocations of HBI, **1**, and **2**, and (c) the dications of **1** and **2** and the monocation of HBI.

This indicates a great structural change from the ground to the excited state for **3** and **3-OMe** dication. As the emission spectrum for these compounds appears in the same position as those of the planar dications of **1**, **2**, and **2-OMe**, we propose that the ground-state nonplanar dication $\mathbf{DC}_{np}$ of **3** and **3-OMe** reaches a planar conformation in the excited state from which fluorescence takes place. Similar behavior was found for related systems.[55,56]

The fluorescence quantum yields of the dications of **1**, **2**, **3**, **2-OMe**, and **3-OMe** (Table 1) were high and showed only a weak dependence on the solvent properties. Similar results were obtained for the model compounds **5** and **6** (Table 1).

Very different fluorescence behavior was observed for **1**, **2**, and **3** on changing the solvent from strongly acidified acetonitrile to water. In aqueous solution, excitation of the dication led to a red-shifted emission spectrum, with maximum

Scheme 1. Acid–Base Equilibria of 1, 2, 2-OMe, 3, 3-OMe, 5, and 6 (R_1 = H or CH_3, R_2 = H, OH, or OCH_3, R_3 = H, CH_3, or C_2H_5), Showing the Dication (DC),[a] the Monocation (MC), and the Neutral Form (N)[b]

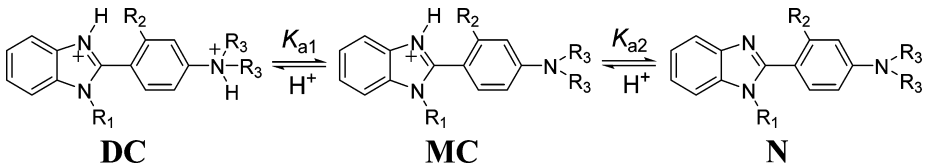

[a]For **3** and **3-OMe**, **DC** has a nonplanar structure. [b]For **1**, **2**, and **3**, the neutral tautomer **T** exists in equilibrium with **N** in neutral aqueous solution. **N** has a nonplanar structure for **3** and **3-OMe** in aqueous solution (see ref 41).

dx.doi.org/10.1021/jp507917u | J. Phys. Chem. B XXXX, XXX, XXX–XXX

at 22000−23000 cm^{-1} and very large Stokes shift (Figure 3). This indicates that the initially excited dication is converted in the excited state to another species, whose fluorescence is detected. This excited-state transformation does not take place for the dications of the methoxy derivatives **2-OMe**, and **3-OMe** (Figure 3b,c).

It is well-known that many phenol derivatives are stronger acids in the excited state. The acidity increase upon excitation is even stronger for cationic species like the monocations of HBI,[34] 2-(3′-hydroxy-2′-pyridyl)benzimidazole,[48] and 2-(1′-hydroxy-2′-naphthyl)benzimidazole,[19,49] protonated at the benzimidazole N3. These species behave as strong photoacids, which deprotonate upon excitation at the hydroxyl group, totally in water and very efficiently in alcohols. We propose that the dications of **1**, **2**, and **3** are also strong photoacids that transfer their hydroxyl proton to water upon excitation to yield the fluorescent tautomeric monocation **TC***, protonated at the benzimidazole N3 and at the amino group, and deprotonated at the hydroxyl group (Scheme 2). This species is a tautomer of the monocation **MC** present in the ground state. As the spectrum of the red-shifted emission of **TC*** is similar for **1**, **2**, and **3**, we assume that **TC*** has the same planar structure for all three species. This implies that excitation of the nonplanar dication of **3**, $\mathbf{DC}_{np}$, is followed by deprotonation and rotational relaxation in the excited state to yield the planar **TC*** form with intramolecular hydrogen bond $O^{-}\cdots H-N$ (Scheme 3).

Scheme 2. Excitation and Deactivation Pathways of the Dications of 1 and 2 in Aqueous Solution[a]

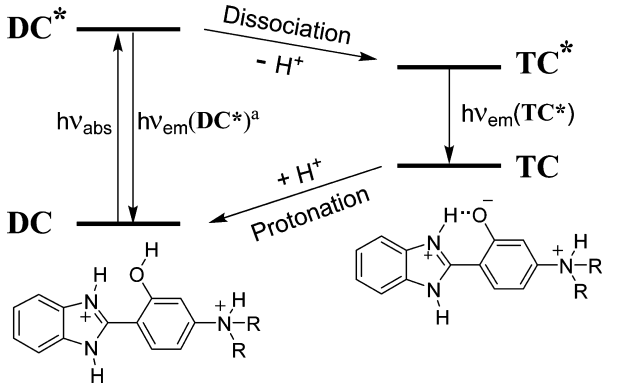

[a]Fluorescence of **DC*** in water detected only for **1**.

The dication of **1** seems to be a weaker photoacid than those of **2** and **3**, as the red-shifted emission of **TC*** is accompanied by a weak shoulder at emission wavenumbers corresponding to the undissociated dication (Figure 3a). This shoulder is not detected in the fluorescence spectra of **2** and **3**.

The emission spectrum of **1**, **2**, and **3** in acidified acetonitrile shows a shoulder at lower wavenumbers that is not detected for **2-OMe** and **3-OMe** and is located at the same position as the emission maximum of **TC*** in water. We suggest that this weak emission corresponds to a small amount of **TC*** formed in acetonitrile, this process being favored by minor amounts of water in this solvent.

Fluorescence decay measurements performed for **2** and **2-OMe** (Table 2) in strongly acidified solvents support the previous assignments. As expected, the fluorescence decay was monoexponential for **2-OMe**. The same lifetime (1.7 ns) is obtained in acetonitrile and in water, which is assigned to **2-OMe DC***. The monoexponential decay obtained for **2** in strongly acidified aqueous solution led to a lifetime value of 3.8 ns, which is assigned to the species **TC*** formed by dissociation of the excited dication. Monoexponential decay was also obtained for **2** in acetonitrile at higher emission wavenumbers, with a lifetime of 1.55 ns attributed to **DC***. This value is similar to that of **2-OMe DC*** (1.7 ns). Biexponential decay was detected for **2** in acetonitrile in the lower-wavenumber region. The second lifetime (4.05 ns) was very similar to the fluorescence lifetime of **TC*** in water (3.8 ns). This result confirms the assignment of the lower-wavenumber shoulder in the emission spectrum of **2** in acetonitrile (Figure 3b) to the fluorescence of **TC***.

4.3. Excited-State Behavior of 1, 2, 3, 2-OMe, 3-OMe, 4, 5, and 6 in Mildly Acidic Solutions: Deactivation of the Monocation MC* by Intramolecular Charge Transfer. For both **1** and **2** in slightly acidic aqueous solution, the fluorescence excitation spectrum matched the absorption spectrum recorded in the same conditions (Figure 4a,b), and therefore, it must be due to the main species present at this acidity, the monocation **MC** protonated at the benzimidazole N3 (Scheme 1). This means that excitation of **MC** gives rise to

Scheme 3. Excitation and Deactivation Pathways of the Dication of 3 in Aqueous Solution

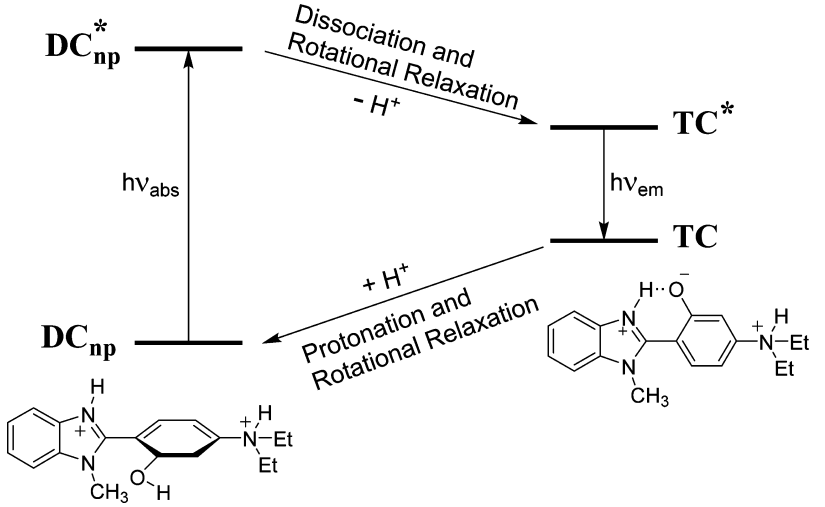

dx.doi.org/10.1021/jp507917u | J. Phys. Chem. B XXXX, XXX, XXX−XXX

Scheme 4. Excitation and Deactivation Pathways of the Monocation of Compounds 6, 2, 2-OMe, 3, and 3-OMe[a]

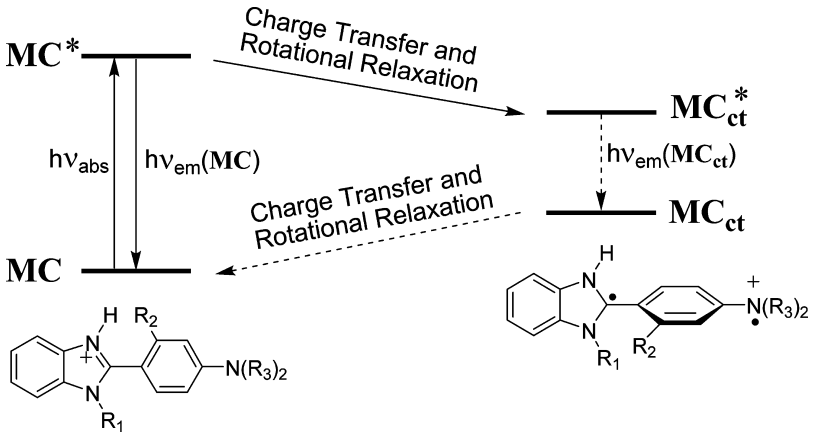

[a]MC^*_{ct} fluoresces slightly for 3 and 3-OMe.

the one-band emission spectrum, which was independent of the excitation wavenumber, and overlapped its excitation spectrum. These results indicate that **MC*** is the fluorescent species. The fluorescence excitation and emission spectra of **1** and **2** in slightly acidified acetonitrile were practically coincident with the spectra measured in water, and the spectra of **2-OMe** were very similar to that of **2** (Figure 4a,b). These results led us to conclude that the monocation MC is the only absorbing and fluorescent species for **1**, **2**, and **2-OMe** in slightly acidified acetonitrile and water.

The above results indicate that the monocations of **1** and **2** do not dissociate in the excited state in water. This behavior is clearly different from that showed by the monocations of the related compounds HBI,[34] 2-(3′-hydroxy-2′-pyridyl)-benzimidazole,[48] and 2-(1′-hydroxy-2′-naphthyl)-benzimidazole.[19,49] For all these compounds, the excited monocation is a strong photoacid that deprotonates at the hydroxyl group to yield the neutral tautomer **T***, totally in water and very efficiently in short-chain alcohols. The fact that the monocations of **1** and **2** do not deprotonate in the excited state must be related to the presence in these compounds of a $-NH_2$ or a $-NEt_2$ group. The charge donation of these groups to the phenol ring must inhibit dissociation at the hydroxyl group, as a consequence of the increase in the excited-state pK_a value of the OH group of **1** and **2** with respect to those of HBI and related compounds lacking the amino group.

The absorption and fluorescence spectra of **3** and **3-OMe** in acidified acetonitrile (Figure 4c) showed the same general features as those of **1**, **2**, and **2-OMe** (Figure 4a,b). The excitation spectrum matched the absorption spectrum of **MC**, and the emission spectrum overlapped its excitation spectrum. This indicates that the emission band of **3** and **3-OMe** is also due to **MC***. However, it is seen that the emission spectra of **3** and **3-OMe** were much broader than those recorded for **1**, **2**, and **2-OMe** (Figure 4a–c). This suggests that the fluorescence of **MC*** is accompanied by the emission of a second species for **3** and **3-OMe**. The identity of this species will be discussed later.

In spite of the similarity between the fluorescence spectrum of monoprotonated **1**, **2**, and **2-OMe**, a close look at the fluorescence quantum yields (Φ_{MC}, Table 3) and lifetime values (τ_1 and τ_2, Table 4) reveals important differences between **1** and its derivatives **2** and **2-OMe**. It is observed in Table 3 that both HBI and its amino derivative **1** showed monocation fluorescence quantum yields in the range 0.24 to 0.36 in all the solvents studied (except **1** in water, Φ_{MC} = 0.10). However, Φ_{MC} values for **2** and **2-OMe** (with a $-NEt_2$ group at C4′) were lower than for **1** and HBI in solvents of high polarity and low viscosity, this effect being stronger for the methylated derivative **2-OMe**.

The fluorescence quantum yields of **3** monocation were lower than that of **2** (Table 3), and the same occurs for **3-OMe** and **2-OMe**. As can be seen in Table 3, Φ_{MC} values were relatively high for **3-OMe** in very viscous solvents (1-octanol, glycerol, ...), but they decreased as solvent viscosity decreased and solvent polarity increased, showing the same behavior as **2** and **2-OMe**.

To investigate the effect of the hydroxyl or methoxy groups of **1**, **2**, **3**, and derivatives on their fluorescence behavior, we studied the model compounds **4**, **5**, and **6**, with no hydroxyl or methoxy substituents at C4′ (Chart 2). The absorption and fluorescence spectra as well as the pK_a values of these compounds in aqueous solution have already been reported.[52,53,57] It has been shown that the first protonation of **4**, **5**, and **6** takes place, like for HBI and its amino and diethylamino derivatives, at the benzimidazole N3 to give monocation **MC**. For **4**, **5**, and **6**, the absorption spectrum of **MC** in acidified acetonitrile and the excitation and emission spectra in the same solvent are shown in Figure 4d. We conclude from these spectra that for the three compounds excitation of **MC** leads to **MC*** fluorescence. However, whereas **MC*** fluorescence quantum yields were high for **4** and **5** and virtually independent of solvent (as for HBI and **1**, see Table 3), the values for **6** drastically decreased with respect to those of **4** and **5**. Moreover, Φ_{MC} values for **6** strongly decreased as the solvent polarity increased and solvent viscosity decreased.

The above results provide compelling evidence that the monocations of **6**, **2**, **2-OMe**, **3**, and **3-OMe** undergo in the excited state a radiationless deactivation process that increases its efficiency as the solvent polarity increases and the solvent viscosity decreases. Moreover, the strong dependence of the process with the solvent viscosity suggests that it involves a large-amplitude motion. Also, as neither the monocations of HBI and **1**, nor those of **4** and **5**, experience that radiationless deactivation, we conclude that the presence of the $-NEt_2$ or $-NMe_2$ substituent at C4′ strongly favors the occurrence of the process. To explain these results, we propose that the radiationless deactivation undergone by the monocations of

dx.doi.org/10.1021/jp507917u | J. Phys. Chem. B XXXX, XXX, XXX–XXX

2, **2-OMe**, **3**, **3-OMe**, and **6** is an intramolecular charge migration, from the diethyl- or dimethylaminophenyl ring (donor) to the protonated benzimidazole moiety (acceptor), connected to a large-amplitude rotational motion (TICT process), to give a nonfluorescent charge-transfer intermediate $\mathbf{MC}^*_{ct}$ (Scheme 4). Moreover, as species **1** does not undergo that process, we can conclude that the aminohydroxyphenyl ring is not a good enough electron donor. An analogous charge-transfer process has been previously reported by us[41] for the neutral tautomer **T*** of compounds **2** and **3** from the deprotonated diethylaminophenol ring to the protonated benzimidazole to give a nonfluorescent charge-transfer intermediate. A similar polarity- and viscosity-dependent photoinduced intramolecular charge transfer coupled to an interannular torsional motion has been proposed for related systems as, for example, hydroxyphenylbenzoxazole and -benzothiazole,[45] [(dimethylamino)phenyl]-methylpyridinium,[58] phenol-pyridinium cation,[59] and hydroxyphenylimidazopyridines.[60,61] Different theoretical and experimental approaches have been used to elucidate the nature of the intramolecular charge transfer processes in these and other donor−acceptor organic molecules.[40,62−66]

Taking into account that the charge-transfer process undergone by **MC*** involves a conformational motion, we would expect the process to be more efficient for **3** and **3-OMe** than for **2** and **2-OMe**, because the steric hindrance of the methyl group at benzimidazole N1 in **3** and **3-OMe** would facilitate the conformational motion needed for the process to take place. A close look at the data in Table 3 reveals that, as expected, Φ_{MC} values were lower for **3** and **3-OMe** than for **2** and **2-OMe**. However, the emission spectrum of **MC*** in acetonitrile was for **3** and **3-OMe** much broader than that recorded for the monocations of **1**, **2**, and **2-OMe** (Figure 4), but it became narrower in very viscous solvents like glycerol (Figure 4c). This suggests that, for the *N*-methyl derivatives, the charge-transfer species might be fluorescent, leading to a broad emission spectrum, comprising the fluorescence of **MC*** and $\mathbf{MC}^*_{ct}$. However, in very viscous solvents, like glycerol, where conformational motion cannot take place, and therefore the process $\mathbf{MC}^* \rightarrow \mathbf{MC}^*_{ct}$ is inhibited, emission is virtually due only to **MC***. Emission from an intramolecular charge-transfer state has been reported for the related compounds dimethylaminophenylimidazopyridines[67−69] and also for the well-known dimethylaminobenzonitrile and related species.[70]

Additionally, it is observed in Table 3 that Φ_{MC} values were clearly lower for **2-OMe** than for **2**. This is also in agreement with our interpretation of the results, because the methoxy group in **2-OMe** slightly improves the strength of the electron donor, and therefore the charge-transfer efficiency is higher for **2-OMe** than for **2**. As deduced from the values in Table 3, this effect is not significant for **3-OMe**, with quantum yields similar to **3**, probably due to the fact that the steric hindrance of the methyl group at benzimidazole N1 in both compounds strongly facilitates the torsional motion connected to the charge transfer.

From the proposed mechanism (Scheme 4), monoexponential fluorescence decays would be expected for the monocations of the investigated compounds. However, fluorescence decays were biexponential for all the compounds except **1** and **5**, and **2** in 1-octanol (see Table 4). For **2**, **2-OMe**, **3-OMe**, and **6** in acetonitrile, the value of lifetime τ_1 (∼1.1 ns) was very similar to that obtained for **1** and **5** (∼1.3 ns), which do not experience the intramolecular charge-transfer process $\mathbf{MC}^* \rightarrow \mathbf{MC}^*_{ct}$, and its contribution increased with the emission wavenumber. Lifetime τ_2 (the shorter times are at the resolution limit of our equipment) tends to be shorter, and its intensity fraction higher, for compounds with lower Φ_{MC} values, indicating its relation to the process $\mathbf{MC}^* \rightarrow \mathbf{MC}^*_{ct}$. In the more viscous solvent 1-octanol, the process $\mathbf{MC}^* \rightarrow \mathbf{MC}^*_{ct}$ should be less efficient than in acetonitrile. In agreement with this, τ_2 values (Table 4) significantly increased on going from acetonitrile to 1-octanol for **2**, **2-OMe**, **3-OMe**, and **6**, and its intensity fraction significantly decreased. For **2**, the fluorescence decay in 1-octanol was monoexponential with a τ_1 value (1.28 ns) very similar to that of **1** and **5** in acetonitrile, indicating that the charge-transfer process is not efficient for **2** in this solvent.

A possible explanation for the above behavior is that **MC*** emission takes place from different multistep relaxation structures. Under this assumption, the observed biexponential fluorescence decay would be a simplification of a nonexponential decay. The complex decay kinetics observed for the monocations here studied has also been found for other charge-transfer molecular rotors, as for example, *p*-(9-anthryl)-*N*,*N*-dimethylaniline,[71] auramine,[72,73] and thioflavin-T.[74] Nonexponential and wavelength-dependent kinetics is a common characteristic for this type of molecules, and several theoretical models were proposed to explain the complex decay.[71−74]

5. CONCLUSIONS

We have shown that the first protonation of compounds **1**, **2**, **3**, **2-OMe**, and **3-OMe** in the ground state takes place at the benzimidazole N3 to give monocation **MC**. The second protonation occurs at the amino group to yield dication **DC** (nonplanar for **3** and **3-OMe**). In acetonitrile, under excitation of **DC**, fluorescence from **DC*** was observed for all these compounds. In aqueous solution, the excited dication **DC*** of **1**, **2**, and **3** behaves as a strong photoacid, deprotonating (totally for **2** and **3**) at the hydroxyl group to yield the fluorescent tautomeric monocation **TC***. This species, protonated at the imidazole and amino nitrogens and deprotonated at the hydroxyl group does not exist in significant amounts in the ground state. After deactivation, **TC** protonates again to regenerate **DC**.

Unlike HBI and some derivatives, the excited monocations of **1**, **2**, and **3** did not deprotonate at the hydroxyl group. The fluorescence from **MC*** was detected for **1**, **2**, and **3**, and their methoxy derivatives in all the solvents investigated. On the other hand, whereas the monocation fluorescence quantum yield of **1** was virtually independent of solvent, those of **2**, **3**, **2-OMe**, **3-OMe**, and the simple model compound **6** showed a viscosity- and polarity-dependent radiationless deactivation associated with a large-amplitude conformational motion undergone by **MC***. We have shown that this rotational motion is connected to an intramolecular charge transfer (TICT) from the phenyl unit to the protonated benzimidazole moiety, to give a charge-transfer structure $\mathbf{MC}^*_{ct}$. Fluorescence from this charge-transfer species could only be detected for **3** and **3-OMe**. The efficiency of this process, not observed for **1**, **4**, and **5**, increased with the strength of the electron-donor group and with the steric hindrance of the methyl group at benzimidazole N1.

AUTHOR INFORMATION

Corresponding Authors

*E-mail: carmen.rios@usc.es.

*E-mail: manuel.mosquera@usc.es.

*E-mail: flor.rodriguez.prieto@usc.es.

Notes

The authors declare no competing financial interest.

■ ACKNOWLEDGMENTS

We are indebted to the European Regional Development Fund, the Spanish Ministry of Economy and Competitiveness (Grant CTQ2010-17835), and the Xunta de Galicia (Grants GPC2013/052, CN2012/314, and EM2012/091) for financial support of our work. S.R. and J.L.P.L. are thankful for a MEC-FPU fellowship and a "Ramón y Cajal" contract, respectively.

■ REFERENCES

(1) Llano, J.; Eriksson, L. A. First Principles Electrochemical Study of Redox Events in DNA Bases and Chemical Repair in Aqueous Solution. *Phys. Chem. Chem. Phys.* **2004**, *6*, 2426−2433.
(2) Borg, O. A.; Eriksson, L. A.; Durbeej, B. Electron-Transfer Induced Repair of 6−4 Photoproducts in DNA: A Computational Study. *J. Phys. Chem. A* **2007**, *111*, 2351−2361.
(3) Sobolewski, A. L.; Domcke, W. Relevance of Electron-Driven Proton-Transfer Processes for the Photostability of Proteins. *ChemPhysChem* **2006**, *7*, 561−564.
(4) Meyer, T. J.; Huynh, M. H. V.; Thorp, H. H. The Possible Role of Proton-Coupled Electron Transfer (PCET) in Water Oxidation by Photosystem II. *Angew. Chem., Int. Ed.* **2007**, *46*, 5284−5304.
(5) Belevich, I.; Verkhovsky, M. I.; Wikstroem, M. Proton-Coupled Electron Transfer Drives the Proton Pump of Cytochrome c Oxidase. *Nature* **2006**, *440*, 829−832.
(6) Weinberg, D. R.; Gagliardi, C. J.; Hull, J. F.; Murphy, C. F.; Kent, C. A.; Westlake, B. C.; Paul, A.; Ess, D. H.; McCafferty, D. G.; Meyer, T. J. Proton-Coupled Electron Transfer. *Chem. Rev.* **2012**, *112*, 4016−4093.
(7) Chipem, F. A. S.; Mishra, A.; Krishnamoorthy, G. The Role of Hydrogen Bonding in Excited State Intramolecular Charge Transfer. *Phys. Chem. Chem. Phys.* **2012**, *14*, 8775−8790.
(8) Demchenko, A. P.; Tang, K.-C.; Chou, P.-T. Excited-State Proton Coupled Charge Transfer Modulated by Molecular Structure and Media Polarization. *Chem. Soc. Rev.* **2013**, *42*, 1379−1408.
(9) Hammes-Schiffer, S.; Soudackov, A. V. Proton-Coupled Electron Transfer in Solution, Proteins, and Electrochemistry. *J. Phys. Chem. B* **2008**, *112*, 14108−14123.
(10) Ko, C.; Solis, B. H.; Soudackov, A. V.; Hammes-Schiffer, S. Photoinduced Proton-Coupled Electron Transfer of Hydrogen-Bonded *p*-Nitrophenylphenol-Methylamine Complex in Solution. *J. Phys. Chem. B* **2013**, *117*, 316−325.
(11) Hsieh, C.-C.; Jiang, C.-M.; Chou, P.-T. Recent Experimental Advances on Excited-State Intramolecular Proton Coupled Electron Transfer Reaction. *Acc. Chem. Res.* **2010**, *43*, 1364−1374.
(12) De Silva, A. P. Luminescent Photoinduced Electron Transfer (PET) Molecules for Sensing and Logic Operations. *J. Phys. Chem. Lett.* **2011**, *2*, 2865−2871.
(13) Tian, H.; Yang, X.; Cong, J.; Chen, R.; Liu, J.; Hao, Y.; Hagfeldt, A.; Sun, L. Tuning of Phenoxazine Chromophores for Efficient Organic Dye-Sensitized Solar Cells. *Chem. Commun.* **2009**, 6288−6290.
(14) Wu, Y.; Zhu, W. Organic Sensitizers from D-π-A to D-A-π-A: Effect of the Internal Electron-Withdrawing Units on Molecular Absorption, Energy Levels and Photovoltaic Performances. *Chem. Soc. Rev.* **2013**, *42*, 2039−2058.
(15) Baranoff, E.; Barigelletti, F.; Bonnet, S.; Collin, J.-P.; Flamigni, L.; Mobian, P.; Sauvage, J.-P. From Photoinduced Charge Separation to Light-Driven Molecular Machines. *Struct. Bonding (Berlin, Ger.)* **2007**, *123*, 41−78.
(16) Agmon, N. Elementary Steps in Excited-State Proton Transfer. *J. Phys. Chem. A* **2005**, *109*, 13−35.
(17) Pérez-Lustres, J. L.; Rodríguez-Prieto, F.; Mosquera, M.; Senyushkina, T. A.; Ernsting, N. P.; Kovalenko, S. A. Ultrafast Proton Transfer to Solvent: Molecularity and Intermediates from Solvation- and Diffusion-Controlled Regimes. *J. Am. Chem. Soc.* **2007**, *129*, 5408−5418.
(18) Veiga-Gutiérrez, M.; Brenlla, A.; Carreira Blanco, C.; Fernández, B.; Kovalenko, S. A.; Rodríguez-Prieto, F.; Mosquera, M.; Pérez Lustres, J. L. Dissociation of a Strong Acid in Neat Solvents: Diffusion Is Observed after Reversible Proton Ejection Inside the Solvent Shell. *J. Phys. Chem. B* **2013**, *117*, 14065−14078.
(19) Brenlla, A.; Veiga Gutiérrez, M.; Ríos Rodríguez, M. C.; Rodríguez-Prieto, F.; Mosquera, M.; Pérez Lustres, J. L. Moderately Strong Photoacid Dissociates in Alcohols with High Transient Concentration of the Proton-Transfer Contact Pair. *J. Phys. Chem. Lett.* **2014**, *5*, 989−994.
(20) Mansueto, E. S.; Wight, C. A. Excited-State Proton-Transfer Polymerization of Amorphous Formaldehyde. *J. Am. Chem. Soc.* **1989**, *111*, 1900−1901.
(21) Silvi, S.; Arduini, A.; Pochini, A.; Secchi, A.; Tomasulo, M.; Raymo, F. M.; Baroncini, M.; Credi, A. A Simple Molecular Machine Operated by Photoinduced Proton Transfer. *J. Am. Chem. Soc.* **2007**, *129*, 13378−13379.
(22) Irie, M. Light-Induced Reversible pH Change. *J. Am. Chem. Soc.* **1983**, *105*, 2078−2079.
(23) Paterson, M. J.; Robb, M. A.; Blancafort, L.; DeBellis, A. D. Mechanism of an Exceptional Class of Photostabilizers: A Seam of Conical Intersection Parallel to Excited State Intramolecular Proton Transfer (ESIPT) in *o*-Hydroxyphenyl-(1,3,5)-triazine. *J. Phys. Chem. A* **2005**, *109*, 7527−7537.
(24) Sobolewski, A. L. Reversible Molecular Switch Driven by Excited-State Hydrogen Transfer. *Phys. Chem. Chem. Phys.* **2008**, *10*, 1243−1247.
(25) Park, S.; Kwon, J. E.; Kim, S. H.; Seo, J.; Chung, K.; Park, S.-Y.; Jang, D.-J.; Medina, B. M.; Gierschner, J.; Park, S. Y. A White-Light-Emitting Molecule: Frustrated Energy Transfer between Constituent Emitting Centers. *J. Am. Chem. Soc.* **2009**, *131*, 14043−14049.
(26) Formosinho, S. J.; Arnaut, L. G. Excited-State Proton Transfer Reactions. II. Intramolecular Reactions. *J. Photochem. Photobiol., A* **1993**, *75*, 21−48.
(27) Ormson, S. M.; Brown, R. G. Excited State Intramolecular Proton Transfer Part 1: ESIPT to Nitrogen. *Prog. React. Kinet.* **1994**, *19*, 45−91.
(28) Waluk, J. *Conformational Analysis of Molecules in Excited States*; Wiley-VCH: New York, 2000.
(29) Williams, D. L.; Heller, A. Intramolecular Proton Transfer Reactions in Excited Fluorescent Compounds. *J. Phys. Chem.* **1970**, *74*, 4473−4480.
(30) Sinha, H. K.; Dogra, S. K. Ground- and Excited-State Prototropic Reactions in 2-(*o*-Hydroxyphenyl)benzimidazole. *Chem. Phys.* **1986**, *102*, 337−347.
(31) Das, K.; Sarkar, N.; Majumdar, D.; Bhattacharyya, K. Excited-State Intramolecular Proton Transfer and Rotamerism of 2-(2′-Hydroxyphenyl)benzimidazole. *Chem. Phys. Lett.* **1992**, *198*, 443−448.
(32) Das, K.; Sarkar, N.; Ghosh, A. K.; Majumdar, D.; Nath, D. N.; Bhattacharyya, K. Excited-State Intramolecular Proton Transfer in 2-(2-Hydroxyphenyl)benzimidazole and -benzoxazole: Effect of Rotamerism and Hydrogen Bonding. *J. Phys. Chem.* **1994**, *98*, 9126−9132.
(33) Douhal, A.; Amat-Guerri, F.; Lillo, M. P.; Acuna, A. U. Proton Transfer Spectroscopy of 2-(2′-Hydroxyphenyl)imidazole and 2-(2′-Hydroxyphenyl)benzimidazole Dyes. *J. Photochem. Photobiol., A* **1994**, *78*, 127−138.
(34) Mosquera, M.; Penedo, J. C.; Ríos Rodríguez, M. C.; Rodríguez-Prieto, F. Photoinduced Inter- and Intramolecular Proton Transfer in Aqueous and Ethanolic Solutions of 2-(2′-Hydroxyphenyl)-benzimidazole: Evidence for Tautomeric and Conformational Equilibria in the Ground State. *J. Phys. Chem.* **1996**, *100*, 5398−5407.
(35) Ríos, M. A.; Ríos, M. C. Ab Initio Study of the Hydrogen Bond and Proton Transfer in 2-(2′-Hydroxyphenyl)benzothiazole and 2-(2′-Hydroxyphenyl)benzimidazole. *J. Phys. Chem. A* **1998**, *102*, 1560−1567.
(36) Tsai, H.-H. G.; Sun, H.-L. S.; Tan, C.-J. TD-DFT Study of the Excited-State Potential Energy Surfaces of 2-(2′-Hydroxyphenyl)-

benzimidazole and Its Amino Derivatives. *J. Phys. Chem. A* **2010**, *114*, 4065−4079.
(37) Konoshima, H.; Nagao, S.; Kiyota, I.; Amimoto, K.; Yamamoto, N.; Sekine, M.; Nakata, M.; Furukawa, K.; Sekiya, H. Excited-State Intramolecular Proton Transfer and Charge Transfer in 2-(2′-Hydroxyphenyl)benzimidazole Crystals Studied by Polymorphs-Selected Electronic Spectroscopy. *Phys. Chem. Chem. Phys.* **2012**, *14*, 16448−16457.
(38) Furukawa, K.; Yamamoto, N.; Nakabayashi, T.; Ohta, N.; Amimoto, K.; Sekiya, H. Changes in the Electric Dipole Moments and Molecular Polarizabilities of Enol and Keto Forms of 2-(2′-Hydroxyphenyl)benzimidazole Along the Proton Transfer Reaction Path in a PMMA Film. *Chem. Phys. Lett.* **2012**, *539*−*540*, 45−49.
(39) Chipem, F. A. S.; Behera, S. K.; Krishnamoorthy, G. Enhancing Excited State Intramolecular Proton Transfer in 2-(2′-Hydroxyphenyl)benzimidazole and Its Nitrogen-Substituted Analogues by β-Cyclodextrin: The Effect of Nitrogen Substitution. *J. Phys. Chem. A* **2013**, *117*, 4084−4095.
(40) Chipem, F. A. S.; Krishnamoorthy, G. Comparative Theoretical Study of Rotamerism and Excited State Intramolecular Proton Transfer of 2-(2′-Hydroxyphenyl)benzimidazole, 2-(2′-Hydroxyphenyl)imidazo[4,5-*b*]pyridine, 2-(2′-Hydroxyphenyl)-imidazo[4,5-*c*] pyridine and 8-(2′-Hydroxyphenyl)purine. *J. Phys. Chem. A* **2009**, *113*, 12063−12070.
(41) Ríos Vázquez, S.; Ríos Rodríguez, M. C.; Mosquera, M.; Rodríguez-Prieto, F. Rotamerism, Tautomerism, and Excited-State Intramolecular Proton Transfer in 2-(4′-*N*,*N*-Diethylamino-2′-hydroxyphenyl)benzimidazoles: Novel Benzimidazoles Undergoing Excited-State Intramolecular Coupled Proton and Charge Transfer. *J. Phys. Chem. A* **2008**, *112*, 376−387.
(42) Rodembusch, F. S.; Leusin, F. P.; Campo, L. F.; Stefani, V. Excited State Intramolecular Proton Transfer in Amino 2-(2′-Hydroxyphenyl)benzazole Derivatives: Effects of the Solvent and the Amino Group Position. *J. Lumin.* **2007**, *126*, 728−734.
(43) Rodríguez Prieto, F.; Ríos Rodríguez, M. C.; Mosquera Gonzalez, M.; Ríos Fernandez, M. A. Ground- and Excited-State Tautomerism in 2-(3′-Hydroxy-2′-pyridyl)benzimidazole. *J. Phys. Chem.* **1994**, *98*, 8666−8672.
(44) Chipem, F. A. S.; Dash, N.; Krishnamoorthy, G. Role of Nitrogen Substitution in Phenyl Ring on Excited State Intramolecular Proton Transfer and Rotamerism of 2-(2′-Hydroxyphenyl)-benzimidazole: A Theoretical Study. *J. Chem. Phys.* **2011**, *134*, 104308.
(45) Ríos Vázquez, S.; Ríos Rodríguez, M. C.; Mosquera, M.; Rodríguez-Prieto, F. Excited-State Intramolecular Proton Transfer in 2-(3′-Hydroxy-2′-pyridyl)benzoxazole. Evidence of Coupled Proton and Charge Transfer in the Excited State of Some *o*-Hydroxyarylbenzazoles. *J. Phys. Chem. A* **2007**, *111*, 1814−1826.
(46) Levitt, J. A.; Kuimova, M. K.; Yahioglu, G.; Chung, P.-H.; Suhling, K.; Phillips, D. Membrane-Bound Molecular Rotors Measure Viscosity in Live Cells via Fluorescence Lifetime Imaging. *J. Phys. Chem. C* **2009**, *113*, 11634−11642.
(47) Kuimova, M. K. Mapping Viscosity in Cells Using Molecular Rotors. *Phys. Chem. Chem. Phys.* **2012**, *14*, 12671−12686.
(48) Mosquera, M.; Ríos Rodríguez, M. C.; Rodríguez-Prieto, F. Competition between Protonation and Deprotonation in the First Excited Singlet State of 2-(3′-Hydroxy-2′-pyridyl)benzimidazole in Acidic Solutions. *J. Phys. Chem. A* **1997**, *101*, 2766−2772.
(49) Brenlla, A.; Rodríguez-Prieto, F.; Mosquera, M.; Ríos, M. A.; Ríos Rodríguez, M. C. Solvent-Modulated Ground-State Rotamerism and Tautomerism and Excited-State Proton-Transfer Processes in *o*-Hydroxynaphthylbenzimidazoles. *J. Phys. Chem. A* **2009**, *113*, 56−67.
(50) Crosby, G. A.; Demas, J. N. Measurement of Photoluminescence Quantum Yields. Review. *J. Phys. Chem.* **1971**, *75*, 991−1024.
(51) Melhuish, W. H. Quantum Efficiencies of Fluorescence of Organic Substances: Effect of Solvent and Concentration of the Fluorescent Solute. *J. Phys. Chem.* **1961**, *65*, 229−235.
(52) Dey, J.; Dogra, S. K. Dual Fluorescence of 2-[4-(Dimethylamino)phenyl]benzothiazole and Its Benzimidazole Analog: Effect of Solvent and pH on Electronic Spectra. *J. Phys. Chem.* **1994**, *98*, 3638−3644.
(53) Mishra, A. K.; Dogra, S. K. Effect of Solvents and pH on the Absorption and Fluorescence Spectra of 2-Phenylbenzimidazole. *Spectrochim. Acta* **1983**, *39A*, 609−611.
(54) Weinberg, N. L.; Weinberg, H. R. Electrochemical Oxidation of Organic Compounds. *Chem. Rev.* **1968**, *68*, 449−523.
(55) Ríos Rodríguez, M. C.; Rodríguez-Prieto, F.; Mosquera, M. Conformational Effects on the Photoinduced Proton-Transfer Processes in 1-Methyl-2-(3′-hydroxy-2′-pyridyl)benzimidazole. *Phys. Chem. Chem. Phys.* **1999**, *1*, 253−260.
(56) Rodríguez-Prieto, F.; Penedo, J. C.; Mosquera, M. Solvent Control of Molecular Structure and Excited-State Proton-Transfer Processes of 1-Methyl-2-(2′-hydroxyphenyl)benzimidazole. *J. Chem. Soc., Faraday Trans.* **1998**, *94*, 2775−2782.
(57) Mishra, A. K.; Dogra, S. K. Effects of Solvents and pH on the Spectral Behavior of 2-(*p*-Aminophenyl)benzimidazole. *Bull. Chem. Soc. Jpn.* **1985**, *58*, 3587−3592.
(58) Fromherz, P.; Heilemann, A. Twisted Internal Charge-Transfer in (Aminophenyl)pyridinium. *J. Phys. Chem.* **1992**, *96*, 6864−6866.
(59) Malval, J. P.; Chaumeil, H.; Rettig, W.; Kharlanov, V.; Diemer, V.; Ay, E.; Morlet-Savary, F.; Poizat, O. Excited-State Dynamics of Phenol-Pyridinium Biaryl. *Phys. Chem. Chem. Phys.* **2012**, *14*, 562−574.
(60) Brenlla, A.; Veiga, M.; Ríos Rodríguez, M. C.; Mosquera, M.; Rodríguez-Prieto, F. Fluorescence of Methylated Derivatives of Hydroxyphenylimidazopyridine. Resolution of Strongly Overlapping Spectra and a New ESIPT Dye Showing very Efficient Radiationless Deactivation. *Photochem. Photobiol. Sci.* **2011**, *10*, 1622−1636.
(61) Brenlla, A.; Veiga, M.; Pérez Lustres, J. L.; Ríos Rodríguez, M. C.; Rodríguez-Prieto, F.; Mosquera, M. Photoinduced Proton and Charge Transfer in 2-(2′-Hydroxyphenyl)imidazo[4,5-*b*]pyridine. *J. Phys. Chem. B* **2013**, *117*, 884−896.
(62) Carlotti, B.; Consiglio, G.; Elisei, F.; Fortuna, C. G.; Mazzucato, U.; Spalletti, A. Intramolecular Charge Transfer of Push-Pull Pyridinium Salts in the Singlet Manifold. *J. Phys. Chem. A* **2014**, *118*, 3580−3592.
(63) Young, J. W.; Vaquero-Vara, V.; Yi, J. T.; Pratt, D. W.; Moreno-Vargas, G.; Alvarez-Valtierra, L. Using High Resolution Electronic Spectroscopy to Probe the Effects of Ring Twist on Charge Transfer in 2-Phenylindole and *N*-Phenylcarbazole. *Phys. Chem. Chem. Phys.* **2013**, *15*, 10251−10257.
(64) Thomas, J. A.; Young, J. W.; Fleisher, A. J.; Alvarez-Valtierra, L.; Pratt, D. W. Stark-Effect Studies of 1-Phenylpyrrole in the Gas Phase. Dipole Reversal upon Electronic Excitation. *J. Phys. Chem. Lett.* **2010**, *1*, 2017−2019.
(65) Fleisher, A. J.; Bird, R. G.; Zaleski, D. P.; Pate, B. H.; Pratt, D. W. High-Resolution Electronic Spectroscopy of the Doorway States to Intramolecular Charge Transfer. *J. Phys. Chem. B* **2013**, *117*, 4231−4240.
(66) Letrun, R.; Koch, M.; Dekhtyar, M. L.; Kurdyukov, V. V.; Tolmachev, A. I.; Rettig, W.; Vauthey, E. Ultrafast Excited-State Dynamics of Donor-Acceptor Biaryls: Comparison between Pyridinium and Pyrylium Phenolates. *J. Phys. Chem. A* **2013**, *117*, 13112−13126.
(67) Dash, N.; Chipem, F. A.; Krishnamoorthy, G. Encapsulation of 2-(4′-*N*,*N*-Dimethylamino)phenylimidazo[4,5-*b*]pyridine in β-Cyclodextrin: Effect on H-Bond-Induced Intramolecular Charge Transfer Emission. *Photochem. Photobiol. Sci.* **2009**, *8*, 1708−1715.
(68) Dash, N.; Krishnamoorthy, G. Modulation of the Photophysics of 2-(4′-*N*,*N*-Dimethylaminophenyl)imidazo[4,5-*b*]pyridine by Long Chain *N*-Alkylations. *Photochem. Photobiol. Sci.* **2011**, *10*, 939−946.
(69) Mishra, A.; Sahu, S.; Dash, N.; Behera, S. K.; Krishnamoorthy, G. Double Proton Transfer Induced Twisted Intramolecular Charge Transfer Emission in 2-(4′-*N*,*N*-Dimethylaminophenyl)imidazo[4,5-*b*]pyridine. *J. Phys. Chem. B* **2013**, *117*, 9469−9477.
(70) Grabowski, Z. R.; Rotkiewicz, K.; Rettig, W. Structural Changes Accompanying Intramolecular Electron Transfer: Focus on Twisted Intramolecular Charge-Transfer States and Structures. *Chem. Rev.* **2003**, *103*, 3899−4031.

(71) Siemiarczuk, A.; Ware, W. R. Complex Excited-State Relaxation in *p*-(9-Anthryl)-*N*,*N*-Dimethylaniline Derivatives Evidenced by Fluorescence Lifetime Distributions. *J. Phys. Chem.* **1987**, *91*, 3677−3682.
(72) Van der Meer, M. J.; Zhang, H.; Glasbeek, M. Femtosecond Fluorescence Upconversion Studies of Barrierless Bond Twisting of Auramine in Solution. *J. Chem. Phys.* **2000**, *112*, 2878−2887.
(73) Rafiq, S.; Sen, P. Spectroscopic Evidence of the Presence of an Activation Barrier in the Otherwise Barrierless Excited State Potential Energy Surface of Auramine-O: A Femtosecond Fluorescence Up-Conversion Study. *J. Chem. Phys.* **2013**, *139*, 124302.
(74) Amdursky, N.; Erez, Y.; Huppert, D. Molecular Rotors: What Lies Behind the High Sensitivity of the Thioflavin-T Fluorescent Marker. *Acc. Chem. Res.* **2012**, *45*, 1548−1557.
(75) Marcus, Y. *The Properties of Solvents*; John Wiley & Sons: Chichester, 1998.
(76) Lide, D. R. *Handbook of Chemistry and Physics:A Ready-Reference of Chemical and Physical Data*; 85th ed.; CRC Press LLC: Boca Raton, FL, 2004.
(77) Katritzky, A. R. *Handbook of Heterocyclic Chemistry*; Pergamon Press: New York, 1985.

dx.doi.org/10.1021/jp507917u | *J. Phys. Chem. B* XXXX, XXX, XXX−XXX